

Polarimetric interferometer for measuring nonlinearity error of heterodyne interferometric displacement system

Su'an Xu (许素安)^{1*}, Luc Chassagne², Suat Topcu², Le Chen (陈乐)¹,
Jian Sun (孙坚)¹, and Tianhong Yan (严天宏)¹

¹College of Mechanical and Electrical Engineering, China Jiliang University, Hangzhou 310018, China

²LISV, University of Versailles Saint-Quentin, Versailles Cedex, 78035, France

*Corresponding author: zjxusuan@126.com

Received November 14, 2012; accepted February 25, 2013; posted online May 30, 2013

This letter presents a polarimetric interferometer (PI) that can measure the ellipsometric parameter θ with an accuracy of 0.01° leading to a potential accuracy of 17 pm. The PI is constructed and compared with a commercial heterodyne interferometer (HI). Given its low nonlinearity, the PI is used to measure the residual nonlinearity of a heterodyne interferometric displacement system. A rotating half-wave plate is used to compensate for a part of the nonlinearity error caused by the misalignment of the axis between input polarizing states and beamsplitter.

OCIS codes: 120.2130, 060.4370, 060.2840, 000.3110.

doi: 10.3788/COL201311.061201.

The production of semiconductors, photolithography steppers, and metrological instruments rely on interferometric displacement systems to improve position accuracy. Reduced minimum feature size and increased displacement range in industry impose more stringent performance requirements for interferometric systems. Considering its high signal-to-noise ratio (SNR) and easy alignment, heterodyne interferometers (HIs) are widely used in precision length measurement and positioning systems. However, the accuracy of HIs is limited by their intrinsic nonlinearity error. The methods for measuring or reducing the nonlinearity error of displacement measurements by HIs have been studied by numerous researchers^[1–12]. Wu *et al.*^[1–3] constructed detailed mathematical models of nonlinearity errors in HIs. Lorient *et al.*^[4] developed two independent methods for measuring the polarization state properties of laser beams to determine the non-linearity error in HIs. Wu *et al.*^[5–7], developed specific interferometers without frequency mixing. In 2006, Hou^[8] found that the nonlinearity of HIs could be subdivided by the multiple of the optical path. Her research group^[9] developed a simple technique for eliminating the nonlinearity of a HI using a simple phase compensation system with a rotated polarizer before the detector. Patterson *et al.*^[10] experimentally demonstrated that the nonlinearity error could be reduced by subtracting a small amount of the reference signal from the measurement signal. Eom *et al.*^[11] developed a phase-encoding electronics capable of compensating for the nonlinearity error in HIs.

In this letter, a polarimetric interferometer (PI) capable of interpolating the optical fringe into 1/36 000 using polarization state measurement is proposed. The proposed PI is constructed and compared with a commercial HI by measuring the displacement of the same target mirror. The latter is displaced stepwise with a step value of 20 nm using a high-accuracy position control method. The PI is calibrated with a commercial capacitive sensor equipped with a piezoelectric (PZT) nano-positioning system, and its nonlinearity is approximately 0.5 nm.

Given its low nonlinearity, the proposed PI is considered as a reference for detecting the residual nonlinearity of a heterodyne interferometric displacement system. We also show that a rotating half-wave plate can be used to compensate for a part of the nonlinearity error caused by the misalignment of the axis between input polarizing states and beamsplitter by monitoring the intensities of the residual optical beat signal in the HI. Only one cycle with residual nonlinearity error of approximately 3.5 nm in the heterodyne interferometric displacement system is achieved.

An ideal HI with two orthogonal linearly polarized laser beams and different frequencies (f_1, f_2) is illustrated in Fig. 1. The waves are supposed to propagate along the positive direction of the z -axis of an s - p - z orthogonal coordinate system. The electric field components of the laser beam are as follows. The initial phase is omitted here to simplify the calculation.

$$\begin{cases} E_s = A \exp[-i(2\pi f_2 t)] \\ E_p = B \exp[-i(2\pi f_1 t)] \end{cases}, \quad (1)$$

where A and B are the amplitudes. According to the principle of the HI, the intensity of the reference signal from the photodetector PD1 is

$$I_{\text{ref}} \propto AB \cos(2\pi \Delta f t), \quad (2)$$

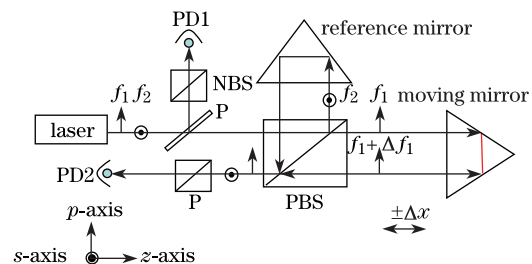


Fig. 1. Principle of the HI. P: polarizer; PBS: polarizing beam splitter; PD: photodetector.

where Δf is the frequency difference between f_2 and f_1 .

In reality, the measurement and reference arms are not pure frequency states. The amplitude of the leakage terms in each arm are denoted as α and β . Considering the effect of frequency mixing, the electric fields of photodetector PD2 contain nonlinearity factors as

$$\begin{cases} E_s = A \exp[-i(2\pi f_2 t + \phi_1)] + \beta \exp[-i(2\pi f_1 t + \phi_1)] \\ E_p = B \exp[-i(2\pi f_1 t + \phi_2)] + \alpha \exp[-i(2\pi f_2 t + \phi_2)] \end{cases}, \quad (3)$$

where ϕ_1 and ϕ_2 are the variations in the phase after the laser beam passes through the reference and measuring paths, respectively. The intensity of the measuring signal from the photodetector PD2 is

$$\begin{aligned} I_{\text{mes}} &\propto AB \cos(2\pi\Delta f t + \phi) \\ &+ (A\beta + B\alpha) \cos(2\pi\Delta f t) \\ &+ \alpha\beta \cos(2\pi\Delta f t - \phi), \end{aligned} \quad (4)$$

where $\phi = \phi_1 - \phi_2$ for a $\pi/2$ phase shift. Equation (4) is expressed in terms of the angle $2\pi\Delta f t$ near zero crossing. The normalized I is

$$I_{\text{mes}} \propto \sin(2\pi\Delta f t) + \left(\frac{\alpha}{A} + \frac{\beta}{B}\right) \cos(2\pi\Delta f t), \quad (5)$$

where the term to the second order in α and β is omitted. The zero crossing shifts by

$$\psi = \tan^{-1} \left(\frac{\alpha}{A} + \frac{\beta}{B} \right). \quad (6)$$

The remaining cosine oscillation in Eq. (5) beats at the Doppler shift frequency. Given the first-order frequency mixing ($\alpha < A, \beta < B$), the nonlinearity value ψ can be expressed as

$$\psi = \frac{\alpha}{A} + \frac{\beta}{B}. \quad (7)$$

The coupling ratios α/A and β/B are the square roots of the ratios of the intensities of the leakage component in the measurement (reference) arm to that of the reference (measurement) arm, which are denoted as $I_{(\alpha/A)}$ and $I_{(\beta/B)}$, respectively. Thus, the nonlinearity can be obtained as

$$\psi = \sqrt{I_{(\alpha/A)}} + \sqrt{I_{(\beta/B)}}. \quad (8)$$

The setup of our PI is shown in Fig. 2. The laser has only one component oriented at 45° with respect to the

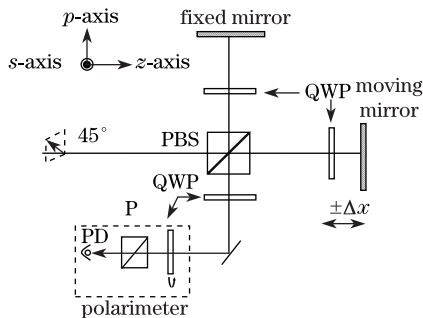


Fig. 2. Schematic representation of the improved homodyne interferometer.

p -axis. The beamsplitter splits the laser light into two beams. Each beam is reflected by fixed and moving mirrors and covers a different path Δl . Quarter-wave plates (QWPs) are used to rotate the polarization of the beams to 90° . At the output of the interferometer, two circularly polarized components with a phase difference equal to $\pm\phi$, depending on the sense of the displacement, are obtained. Each polarized component of the electromagnetic field can be expressed as

$$E_p = \frac{1}{\sqrt{2}} \begin{pmatrix} 1 \\ -i \end{pmatrix}, \quad (9)$$

$$E_s = \frac{1}{\sqrt{2}} \exp(\pm i\phi) \begin{pmatrix} 1 \\ i \end{pmatrix}. \quad (10)$$

At the output of interferometer, the two circularly polarized is combined resulting in a linearly polarized light. This linearly polarized light is sent into a polarimeter, with an electromagnetic field of^[13,14]

$$E = E_p + E_s = \begin{pmatrix} \cos \phi \\ \mp \sin \phi \end{pmatrix} = \begin{pmatrix} \cos \theta \\ \sin \theta \end{pmatrix}, \quad (11)$$

where θ is the angle between the polarization plane and s -axis (Fig. 3).

Equation (11) indicates that the resulting polarization state of the electromagnetic field is linear and rotates with the angle θ about the s -axis as θ varies, i.e., as the mirror moves. Thus, the displacement Δx of the moving mirror to the parameter θ is

$$\Delta x = \frac{\lambda\theta}{2\pi}, \quad (12)$$

where λ is the wavelength in air. The accuracy of θ is normally 0.01° with commercially available polarimeter. Hence, an optical fringe can be interpolated by one part in 36 000. A potential accuracy of $\lambda/72\ 000$ is obtained for a one pass interferometer, which is approximately 17 pm for $\lambda=633$ nm.

A commercial HI (ZMI2001, Zygo, USA) is used in our displacement system. The experimental setup is depicted in Fig. 4. The method of displacement control is completely described in Refs. [15,16] and summarized as follows.

A digital signal generator produces two synchronized signals S_1 and S_2 at the same frequency of 20 MHz. Signal S_1 is sent to the laser head to phase-lock voltage-controlled oscillator (VCO) in the laser head. Signal S_2 is sent to a mixer for phase comparison with signal S_3 , which originates from the output of the interferometer. Signal S_3 contains position information and compared with S_2 . A signal error ε is sent to a phase-locked electronic that pilots the PZT supporting the moving mirror.

In an ideal interferometer, if the target mirror is static, signals S_2 and S_3 are equal in phase. Thus, the resulting signal ε at the mixer is null. If signal S_1 or S_2 undergoes a phase shift by an amount of $\Delta\phi$, signal ε becomes non-null. A motion of the mirror via the lock-in electronic is then generated to compensate for the phase shift by the Doppler shift until phases of S_1 , S_2 , and S_3 become equal.

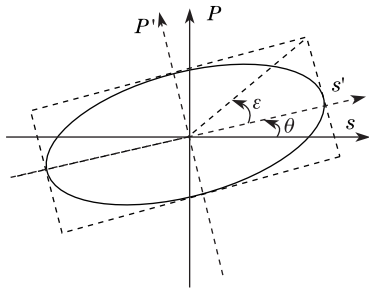
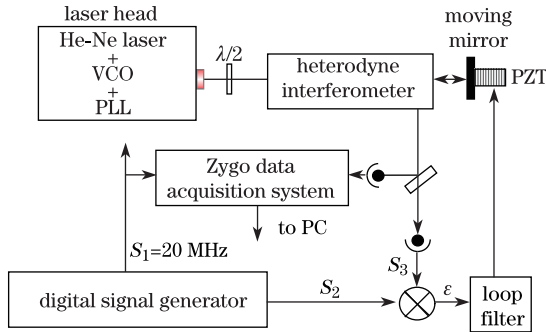
Fig. 3. Definition of the polarimetric parameters ε and θ .

Fig. 4. Principle of the nanodisplacement control using a HI. PLL: phase-locked loop; PC: personal computer.

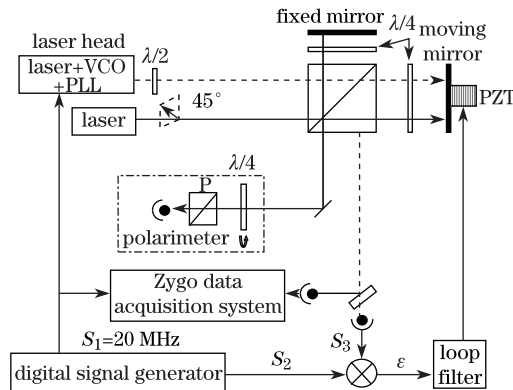


Fig. 5. Experimental setup. The displacement of the target mirror is measured using HI and PI.

If the phase shift is quantified and equal to $\Delta\phi = 2\pi/N$, where N is an integer, the displacement step with a known step value Δx can then be controlled. For a two-pass interferometer, a phase change of 2π corresponds to a displacement of $\lambda/4$, where λ represents the wavelength in air. The displacement step value Δx is related to the phase shift of $\Delta\phi$ by

$$\Delta x = \frac{\lambda\Delta\phi}{8\pi}. \quad (13)$$

The vacuum wavelength is calibrated by the manufacturer, and the value is $\lambda = 632.991528$ nm, with a relative uncertainty of 1.6×10^{-9} . This uncertainty/stability is only relevant when measuring large distances and does not interfere with the effects examined in this study.

The whole nanodisplacement system measured using the HI and PI is mounted on an anti-vibration table, which is less sensitive to mechanical disturbance (Fig.

5). A weather station is installed to simultaneously measure the room temperature (PT100, $1\sigma = 0.01$ °C), pressure (Paroscientific, $1\sigma = 3$ Pa), and humidity content (HygroM4, $1\sigma = 1\%$). The digital signal generator is an AFG3 102 model. The polarimeter used in our system is a spinning QWP polarimeter (PA 450, Thorlabs, USA). The PZT actuator has a displacement range of $3 \mu\text{m}$ for an applied voltage of 30 V.

Considering that the phase shifts of $\Delta\phi = 360^\circ/8 = 45^\circ$ are generated on signal S_2 with a frequency of 1 Hz, the corresponding theoretical displacement step of the PZT actuator is 20 nm based on Eq. (13). The displacement of the same target mirror is simultaneously measured using the HI and PI. The distance between the two beams is less than 10 mm, which has been optimized to avoid some sources of errors such as environmental and mechanical disturbances. The azimuth value θ of the polarized output beam of the PI is measured using a polarimeter. The displacement of the moving mirror is optoelectronically controlled. We first check the two interferometers by measuring the same displacement. The first measure shows a systematic difference from 5 to 7 nm over a displacement distance of $3 \mu\text{m}$, which is the maximum range of our PZT actuator. This difference is due to the translational error of piezo-ceramics. After some adjustment, a suitable reglage for comparing displacement measurements is achieved. The displacements measured with the two interferometers are shown in Fig. 6. The correlation coefficient of the measured values by the two interferometers is equal to 0.9625. The measured values by the two interferometers agree very well. Here, the noise levels at 0.36 nm (1σ) for both interferometers are observed. This noise is essentially induced by the resolution (0.31 nm) of the HI.

In practice, various factors cause the mixed polarization states in both interferometer arms, such as elliptically polarized laser beams, misalignment of axis between input polarizing states and beamsplitter, non-orthogonality in the polarized laser beams, and imperfections of the polarizing beamsplitter. These factors result in the nonlinearity error of the interferometer. As demonstrated by Wu *et al.*^[17,18], the nonlinearity error in a homodyne interferometer roughly depends on the square of the small mixing polarization ratios. By contrast, the error in a HI depends on the large quantity mixing polarization ratios and the sum of these ratios (Eq. (6)). For a polarizing mixing ratio of 0.1, the error

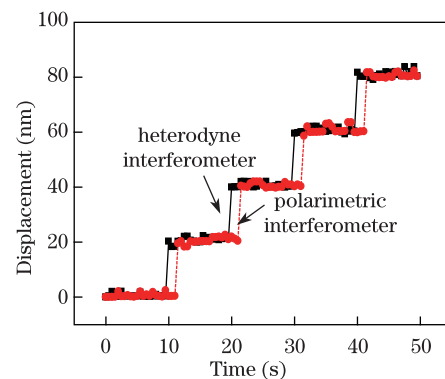


Fig. 6. (Color online) Experimental result of step displacement measured using HI (straight line) and PI (dash line).

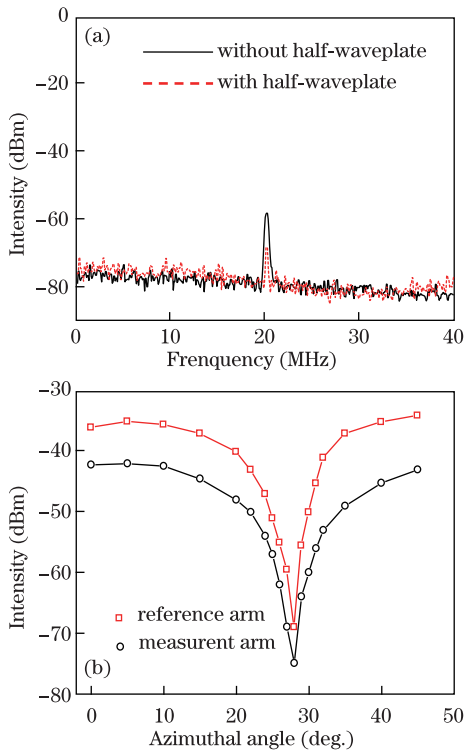


Fig. 7. (Color online)(a) Example of frequency spectrum of the intensity of the 20 MHz residual beat signal in the measurement arm of the HI and (b) recorded values of intensities of the residual optical beat signal for both arms.

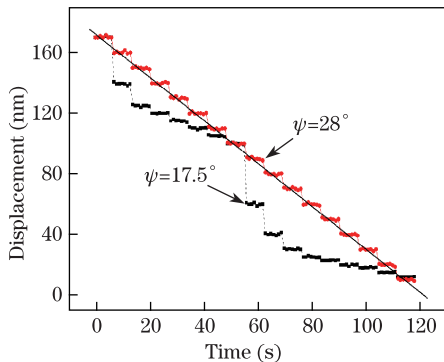


Fig. 8. (Color online) Effect of misalignment of axis between input polarizing states and beamsplitter: straight curve, $\psi = 28^\circ$; dash curve, $\psi = 17.5^\circ$.

in a homodyne interferometer is approximately 20 times smaller than that in a HI. Given that our PI is a homodyne, the nonlinearity in the HI is measured using our PI as a reference.

According to Eqs. (7) and (8), the nonlinearity value of the HI is related to the coupling ratios of the leakage component in the measurement (reference) arm to that of the reference (measurement) arm. According to Hou *et al.*^[19], the polarization directions of laser beams can be adjusted by rotating the half-wave plate based on the assumption that the rotated azimuth angle of $\lambda/2$ plate is α . The two polarization directions then deviate from orthogonality by 2α . The simple rotation of the polarization directions of the laser beam relative to those of the interferometer diminishes the mixed states caused by the

misalignment of the axis between input polarizing states and beamsplitter. We monitor the intensities of the residual optical beat signal with a spectrum analyzer. The output electronic signal of the HI is sent to a spectrum analyzer (Anritsu MS2 661C, Anritsu, USA). During the measurement, one beam travels through, while the other arm is stopped. Initially, the residual beat frequency signal of 20 MHz is observed in the measurement arm at the output of the HI by rotating the half-wave plate. As shown in Fig. 7(a), the intensity of the beat frequency signal reaches its minimum.

The same procedure is conducted for the measurement and reference arms of the HI. The intensities of the residual optical beat signal vary with the azimuthal angle of the half-wave plate for both arms in the HI. The experimental record is depicted in Fig. 7(b). An azimuth angle of the half-wave plate ($\psi = 28^\circ$) is observed, for which the intensities ($I_{(\alpha/A)}$ and $I_{(\beta/B)}$) of residual optical beat signal in our experiment reach the minimum. That is, the sum of the intensities of the residual optical beat signal $\sqrt{I_{(\alpha/A)}} + \sqrt{I_{(\beta/B)}}$ can be minimized. According to Eq. (7), the nonlinearity error is correspondingly diminished, indicating that the nonlinearity error induced by the misalignment of the axis between input polarizing states and beamsplitter can be compensated using a rotating half-wave plate.

An experiment on displacement measurement under different conditions of the azimuthal angle of the half-wave plate is performed. The phase shifts of 22.5° are conducted on signal S_2 , corresponding to position steps of 10 nm. Figure 8 shows the experimental results of the two displacements, in which $\psi = 28^\circ$ corresponds to a minimum coupling ratios case (Fig. 7(b)) and $\psi = 17.5^\circ$ is an example for the case of non-minimum coupling ratios.

Based on Fig. 8, for $\psi = 28^\circ$ (corresponding to the case for minimum coupling ratios), the displacement measure is less affected by nonlinearity compared with those under other azimuth angles. The residual nonlinearity is mainly due to the elliptical polarization of the beam components at the output of the laser head, non-orthogonality in the polarized laser beams, and the imperfections of the polarizing beamsplitter.

To analyze the residual nonlinearity value in the HI, the target mirror is displaced over a range equal to $\lambda = 632.991$ nm. The displacement step value is $\lambda/32 = 20$ nm. The variation in θ is recorded. The experimental results are shown in Fig. 9. The line in the middle represents the ideal value of θ , which is equal to the 11.25° case of non nonlinearity. Figure 9 shows the periodic aspect of the error. The maximum error over one period is equal to 2.25° , corresponding to an error in the displacement of 3.98 nm according to Eq. (12). However, our PI has been calibrated using a capacitive sensor equipped PZT nano-positioning system (Model PI P-621.2CD, Physik Instrumente, Germany). The PZT positioning system has good linearity and dynamic properties. Its linearity is approximately 0.02%, with effective resolution in sub-micron range. Considering the good stability of the PZT nano-positioning system, the nonlinearity of the instrument under test can be directly measured. The calibration procedure is similar to that in Ref. [20]. The target mirror of our PI is mounted on the PZT actuator. A few necessary adjustments of the optical measuring and

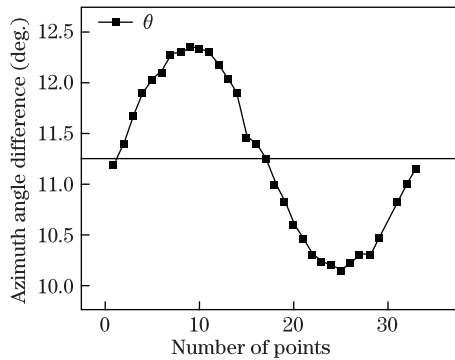


Fig. 9. Measured azimuth angle θ difference of the PI.

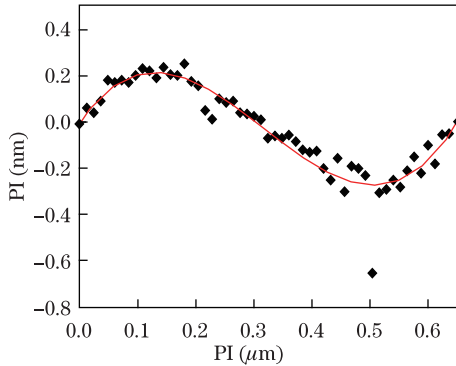


Fig. 10. (Color online) Nonlinearity of our PI.

motion axes of the PZT are conducted to minimize the Abbe error. The displacement of the PZT positioning system is controlled by a personal computer, and the resulting data of the PI can be simultaneously obtained. The nonlinearity of the PI using a commercial PZT positioning system as the reference is shown in Fig. 10. The nonlinearity is only approximately 0.5 nm. Thus, the maximum residual nonlinearity of our heterodyne interferometric system is decreased to 3.5 nm. Furthermore, the nonlinearity error is periodic, and cumulative errors are not observed.

In conclusion, a PI capable of fringe interpolation with an accuracy of one part in 36 000 is presented in this letter. This interferometer is used as a reference for measurement comparison to determine the nonlinearity of our heterodyne interferometric displacement system. To compensate for the nonlinearity caused by the misalignment of the axis between input polarizing states and beamsplitter, a rotatable half-wave plate is placed before the laser head. The variation in the intensity of the residual optical beat signal in each arm of the HI is also monitored. The results show that the effect of the misalignment of the axis between input polarizing states and beamsplitter on periodic error can be minimized for displacement measurement. Based on the measurement and recording of the azimuth angle using a polarimeter (Fig. 10), a peak-to-peak error of up to 3.98 nm is obtained

with a periodicity of one cycle per fringe in optical path length difference. The nonlinearity error of the PI is approximately 0.5 nm (Fig. 10), which is obtained through measurement comparison using a commercial capacitive sensor-equipped PZT nano-positioning system as reference. Therefore, the maximum residual nonlinearity of the HI displacement system is decreased to 3.5 nm. For the position control of the target mirror, the potential accuracy of our PI is $\lambda/72\,000$. The actual accuracy almost reaches the limit of 0.31 nm, which results from the resolution of the commercial HI.

This work was partially supported by the National Natural Science Foundation of China (Nos. 51105348 and 51075377), and the Scientific Research Foundation for the Returned Overseas Chinese Scholars, State Education Ministry.

References

1. C. M. Wu and R. D. Deslattes, *Appl. Opt.* **37**, 6696 (1998).
2. S. J. A. G. Cosijns, H. Haitjema, and P. H. J. Schellekens, *Precis. Eng.* **26**, 448 (2002).
3. W. Lee, J. Lee, and K. You, *Electron. Lett.* **45**, 1085 (2009).
4. D. J. Lorier, B. A. W. H. Knarren, S. J. A. G. Cosijns, H. Haitjema, and P. H. J. Schellekens, *CIRP Annal. Manufact. Technol.* **52**, 439 (2003).
5. C. M. Wu, *Rev. Sci. Instrum.* **79**, 065101 (2008).
6. M. Tnanka, T. Yamagami, and K. Nakayama, *IEEE Trans. Instrum. Meas.* **38**, 552 (1989).
7. J. Lawall and E. Kessler, *Rev. Sci. Instrum.* **71**, 2669 (2000).
8. W. Hou, *Prec. Eng.* **30**, 337 (2006).
9. W. Hou, Y. Zhang, and H. Hu, *Meas. Sci. Technol.* **20**, 105303 (2009).
10. S. Patterson and J. Beckwith, in *Proceedings of the 8th International Precision Engineering Seminar (IPES)* 101 (1995).
11. T. B. Eom, J. A. Kim, C. S. Kang, B. C. Park, and J. W. Kim, *Meas. Sci. Technol.* **19**, 075302 (2008).
12. C. Yin, G. Dai, Z. Chao, Y. Xu, and J. Xu, *Opt. Eng.* **38**, 1361 (1999).
13. S. A. Xu, L. Chassagne, S. Topcu, S. J. Zhong, and Y. Y. Huang, *Sci. China Technol. Sci.* **54**, 3424 (2011).
14. S. Topcu, L. Chassagne, Y. Alayli, and P. Juncar, *Opt. Commun.* **247**, 133 (2005).
15. S. Topcu, L. Chassagne, D. Haddad, and A. Yasser, *Rev. Sci. Instrum.* **74**, 4876 (2003).
16. L. Chassagne, S. Topcu, S. Xu, S. Topcu, P. Ruaux, P. Juncar, and Y. Alayli, *Meas. Sci. Technol.* **18**, 3267 (2007).
17. C. Wu and C. Su, *Meas. Sci. Technol.* **7**, 62 (1996).
18. W. Augustyn and P. Davis, *J. Vac. Sci. Technol. B* **8**, 2032 (1990).
19. W. Hou and G. Wilkening, *Precis. Eng.* **14**, 91 (1992).
20. J. Xu, Y. Xu, and X. Y. Ye, *Acta Metrologica Sinica* (in Chinese) **24**, 271 (2003).